

MLLM IS A STRONG RERANKER: ADVANCING MULTIMODAL RETRIEVAL-AUGMENTED GENERATION VIA KNOWLEDGE-ENHANCED RERANKING AND NOISE-INJECTED TRAINING

Zhanpeng Chen^{21*} Chengjin Xu^{1*} Yiyang Qi¹ Jian Guo^{1†}

¹IDEA Research, International Digital Economy Academy

²School of ECE, Peking University

ABSTRACT

Multimodal Large Language Models (MLLMs) have demonstrated remarkable capabilities in processing and generating content across multiple data modalities, including text, images, audio, and video. However, a significant drawback of MLLMs is their reliance on static training data, leading to outdated information and limited contextual awareness. This static nature hampers their ability to provide accurate, up-to-date responses, particularly in dynamic or rapidly evolving contexts. Integrating Multimodal Retrieval-augmented Generation (Multimodal RAG) offers a promising solution, but the system would inevitably encounter the multi-granularity noisy correspondence (MNC) problem, which involves two types of noise: coarse-grained (query-caption) and fine-grained (query-image). This noise hinders accurate retrieval and generation. In this work, we propose **RagLLaVA**, a novel framework with knowledge-enhanced reranking and noise-injected training, to address these limitations. We instruction-tune the MLLM with a simple yet effective instruction template to induce its ranking ability and serve it as a reranker to precisely filter the top-k retrieved images. For generation, we inject visual noise during training at the data and token levels to enhance the generator’s robustness. Extensive experiments are conducted on the subsets of two datasets that require retrieving and reasoning over images to answer a given query. Our results demonstrate the superiority of RagLLaVA in retrieving accurately and generating robustly. Code and models are available at <https://github.com/IDEA-FinAI/RagLLaVA>.

1 INTRODUCTION

As an attempt towards Artificial General Intelligence (AGI), Large Language Models (LLMs) have made significant strides in language understanding and human-like text generation (Brown et al., 2020; Achiam et al., 2023; Touvron et al., 2023). However, true AGI requires more than just linguistic capabilities. It necessitates a comprehensive understanding and interaction with the world, encompassing multiple modalities beyond text. Thus, the recent progress of Multimodal Large Language Models (MLLM) in handling multimodal information has attracted the community. By processing and generating content across different modalities, MLLMs aim to create a more holistic and nuanced understanding of the world, closer to how humans perceive and interpret information. This integration of modalities enables MLLMs to perform tasks that require contextual understanding from multiple data sources, such as Visual Question Answering (VQA) (Goyal et al., 2017; Hudson & Manning, 2019; Marino et al., 2019; Mishra et al., 2019), Table Question Answering (Lu et al., 2022), Text-to-image Generation (Ramesh et al., 2021; Yu et al., 2022; Aghajanyan et al., 2022), etc.

*Equal contribution.

†Corresponding author.

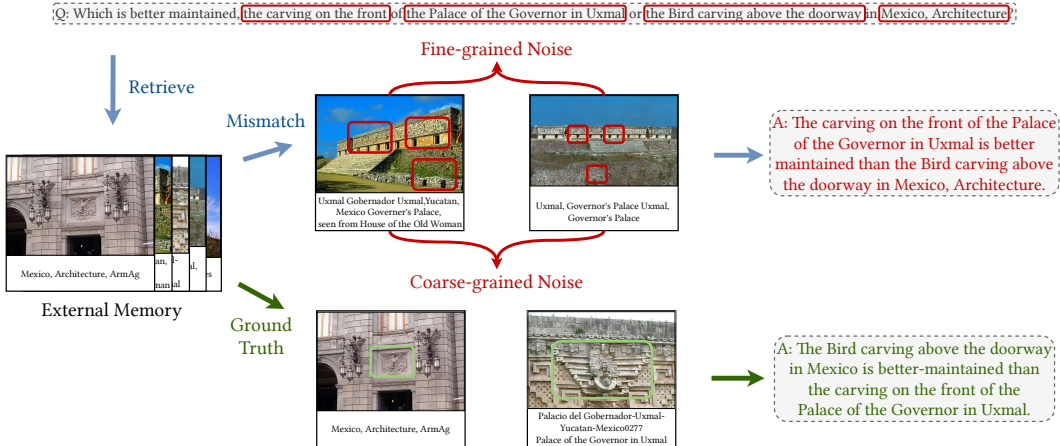


Figure 1: An example from WebQA (Chang et al., 2022) of multi-granularity noisy correspondence (MNC) in multimodal RAG.

Nevertheless, the promising performance of language models primarily relies on the knowledge implicitly stored in their massive parameters, leading to several issues such as long-tail knowledge gaps (Asai et al., 2024), generating hallucinations (Ye & Durrett, 2022), and poor model interpretability. To better adapt to knowledge-intensive tasks and real-world scenarios, Retrieval-augmented Language Models (RALM) (Lewis et al., 2020; Lin et al., 2023; Izacard & Grave, 2020; Karpukhin et al., 2020) employ a dense retriever to retrieve up-to-date knowledge from external memories for grounded generation. Similarly, Multimodal Retrieval-augmented Generation (Multimodal RAG) enhances MLLMs by dynamically retrieving relevant information from external multimodal data sources before the generation process. This allows the models to incorporate real-time, contextually accurate information, significantly improving the factuality and accuracy of their outputs.

As illustrated in Figure 1, to answer the information-seeking query “Which is better maintained, the carving on the front of the Palace of the Governor in Uxmal or the Bird carving above the doorway in Mexico, Architecture?”, the model must retrieve and reason over external visual knowledge, which differs from traditional VQA and is non-trivial. As the first model to extend RAG to multiple modalities, MuRAG (Chen et al., 2022) is built upon ViT (Dosovitskiy et al., 2020) and T5 (Raffel et al., 2020) and pre-trained to encode image-text pairs for both answer generation and retrieval. MuRAG embeds items into an external memory and handles queries for retrieving multimodal knowledge from the same memory. To better connect candidates and model their interdependent relations during retrieval, SKURG (Yang et al., 2023) employs an Entity-centered Fusion Encoder to align sources from different modalities and determines the number of retrieval steps adaptively using a unified Retrieval-generation Decoder.

However, integrating multimodal RAG would inevitably introduce the multi-granularity noisy correspondence problem (MNC) (Huang et al., 2021). As shown in Figure 1, MNC refers to the noise at two different granularities: (I) *Coarse-grained noise (query-caption)*. During the retrieval stage, the retriever needs to search for supporting information relevant to the query from an external memory. In multimodal retrieval, image captions play a crucial role as they provide a summary of the image content, while most image captions offer a coarse-grained description of the image, often lacking detailed information. This results in retrieving similar but negative images (e.g., ‘Uxmal Gobernador Uxmal, Yucatan, Mexico Governor’s Palace, seen from House of the Old Woman’ and ‘Palacio del Gobernador-Uxmal-Yucatan-Mexico0277 Palace of the Governor in Uxmal’ in Figure 1). (II) *Fine-grained noise (query-image)*. Different from coarse-grained noise, fine-grained noise affects both retrieval and generation. On one hand, relying solely on caption information is insufficient for multi-hop questions. The retriever must distinguish fine-grained visual elements among similar images and determine the final recalled images based on the relevance of these elements to the query. On the other hand, the model must formulate responses based on the query and the fine-grained details of the recalled images during generation. The fine-grained noise may originate from irrelevant parts of correctly retrieved images or from incorrectly retrieved images. In this way, any discrepancies

between the images and the question can introduce noise, thereby compromising the accuracy of the generated results.

In this paper, we propose **RagLLaVA**, a novel framework with knowledge-enhanced reranking and noise-injected training, to mitigate multi-granularity noisy correspondence in multimodal RAG. In the retrieval stage, we first utilize CLIP (Radford et al., 2021) to retrieve top- k images from the external memory. To take advantage of image captions and avoid the coarse-grained mismatch, we instruction-tune the MLLM with a simple yet effective instruction template to induce its ranking ability. Given that MLLMs are inherently capable of understanding cross-modal information, we employ the fine-tuned model as a reranker to evaluate the relevance between the query and the image, which precisely selects the top- n candidates that are more related to the query semantically. Subsequently, we apply an adaptive threshold to filter the candidates, collaborating with the reranker to alleviate the fine-grained mismatches. To further mitigate the impact of fine-grained mismatches during the generation phase, we introduce noise at both the data and token levels in the training process. Specifically, at the data level, we perform negative sampling for single-image input questions within the single/multiple-image interleaved dataset, supplementing them with references from hard negative images. At the token level, we introduce additional visual uncertainty to images through Gaussian noise and reassign training loss weights by comparing the logits of the distorted and original inputs. This noise-injected training method effectively enhances the model’s robustness and visual understanding capabilities.

In a nutshell, the main contributions of this work are as follows:

- We achieve effective and robust multimodal retrieval-augmented generation with a three-stage pipeline. Additionally, we address the multi-granularity noisy correspondence (MNC) problem inherent in multimodal retrieval-augmented generation.
- We introduce the knowledge-enhanced reranking and noise-injected training technique to mitigate the coarse-grained and fine-grained noise from MNC.
- Extensive experiments on open-world multimodal question answering tasks demonstrate the effectiveness of the proposed framework.

2 RELATED WORK

2.1 MULTIMODAL LARGE LANGUAGE MODEL

Recent advances in Multimodal Large Language Models (MLLMs) have demonstrated impressive performances in handling multi-format information (Driess et al., 2023; Huang et al., 2024; Achiam et al., 2023). MLLMs are generally built upon existing Large Language Models (LLMs) and integrate visual information as input tokens by utilizing an additional vision encoder (*e.g.* CLIP) and a bridging connector (*e.g.* MLP). For instance, LLaVA (Liu et al., 2024b;a) adopts one/two linear MLP to project visual tokens and align the feature dimension with word embeddings, while BLIP-2 (Li et al., 2023) leverages a group of learnable query tokens to extract information in a query-based manner. However, MM1 (McKinzie et al., 2024) has shown that the number of visual tokens and image resolution are the most critical factors, whereas the type of connector has minimal impact. By connecting the visual and textual modalities, MLLMs significantly enhance human-AI interaction and demonstrate remarkable capabilities in understanding and generating multimodal content. Despite these advances, MLLMs tend to underperform in knowledge-intensive tasks (*e.g.* WebQA and MultimodalQA (Talmor et al., 2021)) that require seeking up-to-date information. Since the knowledge stored in their massive parameters is currently limited, it is crucial for MLLMs to resort to external memories for grounded generation.

2.2 MULTIMODAL RETRIEVAL-AUGMENTED GENERATION

Enhancing language models by incorporating relevant information from diverse knowledge sources has been shown to improve performance across various NLP tasks (Borgeaud et al., 2022; Lewis et al., 2020). DPR (Karpukhin et al., 2020) trains the retriever using in-batch documents and samples negative examples for contrastive learning, allowing the pre-trained retriever to excel in open-domain question answering. REALM (Guu et al., 2020) and RAG (Lewis et al., 2020) treat the retrieved passages as latent variables and train the retriever-generator system jointly, leading to more

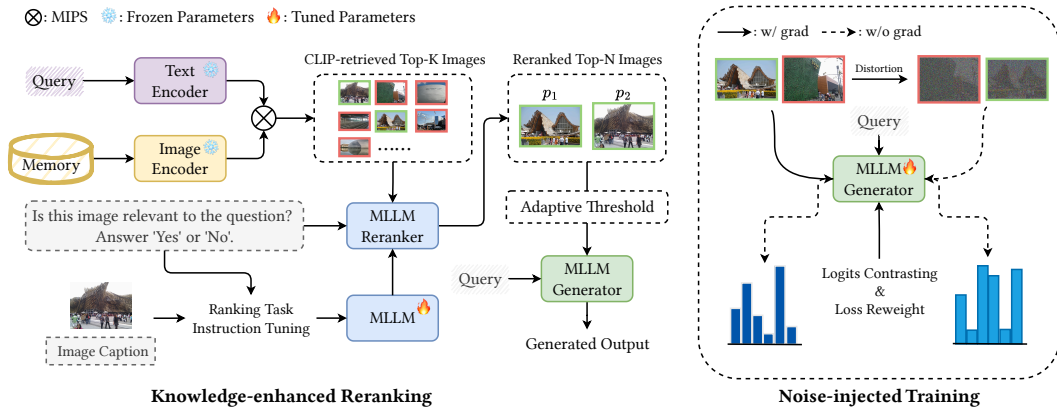


Figure 2: Overview of our proposed RagLLaVA. In the retrieval stage, we utilize the CLIP model and faiss to find the top- K most relevant images through Maximum Inner Product Search (MIPS) (Guo et al., 2020). Subsequently, the highly similar top- K images are reranked into top- N with the fine-tuned MLLM reranker. Finally, the top- N images are fed into the MLLM generator along with the query for accurate generation.

effective retrieval-augmented generation models. Inspired by textual RAG, Plug-and-play (Tiong et al., 2022) retrieves relevant image patches using GradCAM (Selvaraju et al., 2017) to localize relevant parts based on the query. MuRAG (Chen et al., 2022) proposes the first multimodal retrieval-augmented Transformer, which accesses an external non-parametric multimodal memory to augment language generation. However, none of these works specifically focus on MNC in multimodal RAG, which is the primary focus of our research. Experimental results show that the proposed knowledge-enhanced reranking and noise-injected training effectively improves multimodal RAG.

3 METHODOLOGY

3.1 PRELIMINARIES

The traditional Retrieval-augmented Language Model (RALM) acquires knowledge from the external memory \mathcal{M} and utilizes the knowledge in grounded outputs to promote accurate and explainable generation. The retriever \mathcal{R} first retrieves the top- K most relevant contexts $\mathcal{C} = \{c_1, \dots, c_k\}$ from \mathcal{M} for the given question q . Subsequently, the autoregressive language model generates answers based on these retrieved contexts. Under the multimodal setting, the retriever needs to compare the textual queries with the multimodal documents and find the best matches for the generator \mathcal{G} . In this paper, we focus on retrieving the visual-related contexts to study open-world multimodal question answering.

3.2 MULTIMODAL RETRIEVER

We follow the dual-encoder architecture based on CLIP text encoder Φ_{text} and image encoder Φ_{img} . Before the retrieval stage, given image-query pairs (v, q) from the dataset \mathcal{D} , we first apply the image encoder Φ_{img} to encode each image and build the image memory \mathcal{M} using faiss (Douze et al., 2024). From the external memory \mathcal{M} , the retriever aims to retrieve a small set of images that support the textual query q . Specifically, we encode the query with the text encoder Φ_{text} and use MIPS over all of the image candidates $v \in \mathcal{M}$ as follows,

$$\hat{\mathcal{M}} = TopK(\mathcal{M}|q) = TopK_{v \in \mathcal{M}} \Phi_{text}(q) \cdot \Phi_{img}(v). \quad (1)$$

The top- K images with the highest inner product scores, *i.e.* the nearest top- K neighbors $\hat{\mathcal{M}} = \{v_1, v_2, \dots, v_k\}$, are retrieved as the candidate images for answer generation.

3.3 INDUCING RANKING ABILITY OF MLLMS

CLIP stands out across a wide range of multimodal representations and retrieval tasks as a powerful and highly transferable model. However, when encountering long-tail distribution or domain-specific terms, CLIP fails to match the proper pairs across text and images. It results in a higher demand of k value to increase the recall rate of supporting materials, which is time- and resource-consuming. In general, MLLMs are pre-trained on vast image-text pairs for feature alignment and fine-tuned on language-image instruction-tuning datasets for instruction following. With this pre-injected multimodal knowledge, they are inherently capable of understanding semantically relevant contents across both visual and textual modalities. Therefore, to mitigate the bottleneck challenge of multimodal RAG, we introduce a flexible Knowledge-enhanced Ranking task to induce the ranking ability of MLLMs.

Ranking Data Construction To enhance the ranking capability of MLLMs, we construct the instruction-following data based on each multimodal QA dataset. We treat each query and the ground truth images as relevant, while the hard negative images as irrelevant. As shown in Table 1, we construct two types of ranking task and require the model to generate ‘Yes’ for the relevant pairs and ‘No’ for the irrelevant pairs. Intuitively, the caption-aware style brings more additional knowledge for the model to distinguish the relevance between the image and query. Therefore, we train the reranker with the caption-aware ranking task. In addition, the instruction tuning for ranking can be either blended into the supervised fine-tuning of downstream tasks or conducted separately. More analysis of the data organization and instruction template can be seen in §5.2 and §5.3, respectively.

Knowledge-enhanced Reranking By simply asking the question “*Based on the image and its caption, is the image relevant to the question? Answer ‘Yes’ or ‘No’.*”, we measure the relevance between the image and query with the probability p of generating ‘Yes’ calculated from the output logits. Thus, reranking the top- K candidates into top- N can be formulated as follows,

$$\tilde{\mathcal{M}} = \text{Top}N(\hat{\mathcal{M}}|\phi) = \underset{(v,c) \in \hat{\mathcal{M}}}{\text{Top}N} p_\phi(v, c, q), \quad (2)$$

$$p_\phi(v, c, q) = \frac{\exp(\text{logit}(y_1 = \text{“Yes”}|v, c, q))}{\exp(\text{logit}(y_1 = \text{“Yes”}|v, c, q)) + \exp(\text{logit}(y_1 = \text{“No”}|v, c, q))}, \quad (3)$$

where v , c , and q denote the image, corresponding caption, and query, respectively. ϕ is the weight of the reranker. y_1 denotes the first token in the generated output.

Adaptive Threshold Since the reranked images might still have low relevance p to the query, they can negatively affect answer generation, potentially performing worse than not including the images. To further improve the retrieval accuracy, we apply an adaptive threshold η to filter out candidates when $p < \eta$. We set two types of thresholds: the natural threshold and the adaptive threshold. The natural threshold refers to $\eta = 0.5$, which is the natural boundary for our binary classification ranking task. For more precise retrieval, we experiment on the validation set and utilize the intersection point of the interpolated curve of exact match and mismatch as the adaptive threshold. In this way, the model can rely solely on its prior knowledge to answer questions when it cannot retrieve sufficiently relevant images, avoiding the distraction of irrelevant images. By forcing the MLLM to jointly consider the query, caption, and image, the simple yet effective question template stimulates and enhances the model’s ranking ability with multimodal knowledge, thereby supporting the trustworthy generation.

3.4 NOISE-INJECTED TRAINING

Compared to providing a fixed number of images each time, the VQA task with single/multiple images interleaved is more aligned with real-world scenarios. However, it also presents challenges in determining the optimal number of images to provide each time and in extracting relevant information rather than distracting information from the provided images. Though the reranker performs well in selecting relevant images, irrelevant ones still inevitably disturb the accurate generation.

Inspired by VCD (Leng et al., 2024), visual uncertainty amplifies language priors, and contrasting the logits obtained from the enhanced language priors with the original logits can better highlight

Table 1: The instruction template for ranking and generation tasks. The retrieval-augmented QA task allows multi-image input, whereas the ranking tasks consider one image at a time.

| Task | Instruction | Answer |
|-----------------------------------|--|----------|
| Multimodal Retrieval-augmented QA | <image> ... <image> {question} | A phrase |
| Caption-agnostic Ranking | <image> Question:{question} Is this image relevant to the question? Answer ‘Yes’ or ‘No’. | Yes / No |
| Caption-aware Ranking | <image> Image Caption:{caption} Question:{question} Based on the image and its caption, is the image relevant to the question? Answer “Yes” or “No”. | Yes / No |

visual relevance. In light of this, we propose enhancing the model’s robustness by injecting visual noise during training, both at the data level and token level: (I) For single-image/multi-image interleaved datasets, we sample randomly from the hard negatives to ensure that each instruction-following data has the same amount of image input. (II) We introduce additional visual uncertainty by applying a Gaussian noise mask and contrasting the logits to reweight the loss for each token.

Noise-injected Data Construction For datasets that may require both single and multiple image inputs, we standardize the number of image inputs for each sample in the instruction-following data to the maximum number needed for any question. In the case of WebQA, where each question requires 1-2 images for answering, we randomly sample 1 image from the hard negatives as an injected noise for the single-image query. The model is required to distinguish between relevant and irrelevant visual information, which strengthens its capability of visual understanding.

Noise-injected Logits Contrasting Although injecting noise into the dataset can help the model better adapt to noisy environments, it can also be a double-edged sword, making the training process more unpredictable. Instead of the simple Maximum Likelihood Estimation (MLE) loss, we need a more robust objective (Xiao et al., 2024) to guide the model to learn the correlation between visual tokens and textual (query) tokens accurately. We first employ the forward diffusion process (Ho et al., 2020) to distort the image:

$$f(v_t | v_{t-1}) = \mathcal{N}\left(v_t; \sqrt{1 - \gamma}v_{t-1}, \gamma\mathbf{I}\right), f(v_T | v_0) = \prod_{t=1}^T f(v_t | v_{t-1}), \quad (4)$$

where \mathbf{I} and v_0 denote an identity matrix and the original image, respectively. We gradually distort the original image by adding the Gaussian noise for T steps and γ controls the amount of noise added in each step. Subsequently, given a textual query x and an image input v , the model generates two logit distributions conditioned on different visual posteriors: the original v and distorted v^* . By contrasting the logit distributions obtained from these two conditions, we can get the contrastive probability distribution of the i -th sample at time step t as follows,

$$\Delta\text{logit}(y_{i,t}|v_i, v_i^*, x_i, y_{i,<t}) = \text{logit}_\theta(y_{i,t}|v_i, x_i, y_{i,<t}) - \text{logit}_\theta(y_{i,t}|v_i^*, x_i, y_{i,<t}), \quad (5)$$

where $y_{i,t}$ and $y_{i,<t}$ denote the token at time step t and the generated tokens sequence up to the time step $t - 1$ of the i -th sample, respectively. Subsequently, we can obtain the visual correlation weight:

$$\mathbf{w}_{i,t} = \Delta\text{logit}(y_{i,t}|v_i, v_i^*, x_i, y_{i,<t}). \quad (6)$$

Following Xiao et al. (2024) to post-process and smooth the weights, we finally reassign the weight of each token in the vanilla MLE loss, which can be formulated as follows,

$$\mathcal{L}_{INJ}^{i,t} = -\frac{\tilde{\mathbf{w}}_{i,t}}{\sum_{k=1}^l \tilde{\mathbf{w}}_{i,k}} \cdot \text{log}p_\theta(y_{i,t}|v_i, x_i, y_{i,<t}), \quad (7)$$

where l and $\tilde{\mathbf{w}}$ represent the length of textual tokens and the smooth weight, respectively.

Table 2: Performance of reranker on two benchmark datasets. P and R denote precision and recall, respectively. The best scores in each setting are in **bold**.

| Methods | MultimodalQA | | | WebQA | | |
|--|---------------|--------------|--------------|--------------|--------------|--------------|
| | P | R | F1 | P | R | F1 |
| CLIP Top- N | 84.78 | 84.78 | 84.78 | 41.24 | 57.10 | 47.89 |
| <i>Blended Instruction Tuning</i> | | | | | | |
| CLIP Top- K + Reranker | 98.26 | 98.26 | 98.26 | 57.05 | 78.99 | 66.25 |
| w/ Natural Threshold | 100.00 | 97.39 | 98.68 | 67.94 | 78.00 | 72.62 |
| w/ Adaptive Threshold | 100.00 | 97.39 | 98.68 | 84.13 | 62.70 | 71.85 |
| <i>Ranking-only Instruction Tuning</i> | | | | | | |
| CLIP Top- K + Reranker | 98.26 | 98.26 | 98.26 | 57.59 | 79.74 | 66.87 |
| w/ Natural Threshold | 100.00 | 97.83 | 98.90 | 68.31 | 78.52 | 73.06 |
| w/ Adaptive Threshold | 100.00 | 97.83 | 98.90 | 80.38 | 68.35 | 73.88 |

4 EXPERIMENT SETUP

4.1 DATASETS AND EVALUATION METRICS

For evaluation, we consider the image-related subsets of two multimodal QA datasets WebQA and MultimodalQA. Both datasets contain multimodal knowledge-seeking query-answer pairs. Since the test set labels from both datasets are not publicly available, we report the results on the validation set. Each query is associated with a set of hard negative distractors so that two evaluation setups can be used, namely distractor and full-wiki. However, we only consider the full-wiki setting to demonstrate the superiority of our *retrieval-rerank-generation* pipeline.

WebQA consists of queries requiring 1-2 images or text snippets, while 44% of image-based and 99% of text-based queries need multiple knowledge sources. Following the vanilla evaluation setting, we measure the overlap of key entities between the generated output and ground truth answer as *Accuracy*.

MultimodalQA contains multimodal questions over tables, text, and images. We focus on the QA pairs requiring only image information, which are annotated as ‘ImageQ’ and attached to 1 image each. The evaluation metric used is Exact Match (*EM*).

4.2 IMPLEMENTATION DETAILS

This paper uses LLaVA-v1.5-13B (Liu et al., 2024a) as the backbone to evaluate our proposed pipeline. We employ the frozen CLIP-ViT-L/14-336px as the vision and text encoder. For *RagLLaVA*, we first train the reranker model with the ranking task only. Subsequently, we use CLIP to retrieve top- K candidates and rerank them into top- N with the fine-tuned reranker. K is set to 20, while N is set to 2 for WebQA and 1 for MultimodalQA. During instruction tuning, we use LoRA (Hu et al., 2021) and set the learning rate to $2e^{-5}$ following the original setting. We set the batch size to 16 for training the reranker and 8 for the generator. For evaluation, we use greedy decoding to ensure reproducibility and report the best performance. All experiments are conducted on 8 40G NVIDIA A100 GPUs.

5 EXPERIMENTS AND ANALYSIS

5.1 MAIN RESULTS

Results of Retrieval As shown in Figure 3, we collect the relevance probability of the image candidates after reranking and the results prove the superiority of our proposed knowledge-enhanced reranking. Among the train, validation, and test sets, the relevance probabilities of correct recalls are concentrated in the highest range. Since there is still a portion of erroneous recalls whose relevance probabilities are relatively high, we plotted the interpolated curves of correct recalls and erroneous recalls on the validation set and took the x-coordinate of their intersection point as the adaptive

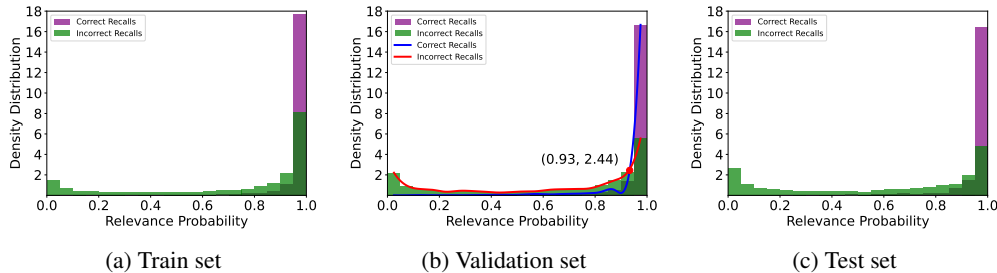


Figure 3: Density distribution of the relevance probability of correct and incorrect recalls on WebQA after reranking. The reranker is instruction-tuned exclusively with the ranking task.

Table 3: Performance of multimodal question answering on two benchmark datasets requiring image retrieval. In addition to the overall results, we report the accuracy of single-image and multi-image input with *Single.* and *Multi.* for WebQA, respectively. *Oracle* refers to directly feeding the ground truth image to the generator. The best scores in each training setting are in **bold**.

| Methods | MultimodalQA | | WebQA | |
|--|--------------|--------------|--------------|--------------|
| | EM | Single. | Multi. | Overall |
| <i>w/o Instruction Tuning</i> | | | | |
| Oracle | 76.96 | 50.58 | 51.10 | 50.81 |
| RagLLaVA | 76.09 | 41.79 | 50.62 | 45.72 |
| w/ Natural Threshold | 76.96 | 46.01 | 50.86 | 48.17 |
| w/ Adaptive Threshold | 76.96 | 46.39 | 50.97 | 48.43 |
| <i>Noise-injected Instruction Tuning</i> | | | | |
| Oracle | 77.39 | 65.51 | 77.04 | 70.63 |
| RagLLaVA | 76.96 | 57.06 | 76.18 | 65.56 |
| w/ Natural Threshold | 77.83 | 60.86 | 76.83 | 67.95 |
| w/ Adaptive Threshold | 77.83 | 61.76 | 76.90 | 68.49 |

threshold. Due to the perfect performance on MultimodalQA with the natural threshold, we set the adaptive threshold to the same as the natural threshold.

As demonstrated in Table 2, our proposed knowledge-enhanced reranking method demonstrates superior performances. We train the reranker under two settings: (i) Blended training of ranking and QA tasks. (ii) Training exclusively with the ranking task. Whether training with the blended or separate setting, our approach achieves better performance across all metrics compared to directly using CLIP for top-N retrieval. When the adaptive threshold η is activated, the model accurately filters out irrelevant images, resulting in improved *accuracy* and *F1* score. Specifically, in WebQA, when η is set to an intuitively reasonable value of 0.5, the corresponding F1 score increases by 25.17% after training on the ranking-only task. In MultimodalQA, the reranker successfully identifies all ground truth images from the retrieved top- K candidates when η is set to 0.5, proving the strong capability of our proposed method in retrieval reranking.

Table 4: Ablation study on WebQA. *NLC* and *ND* refer to Noise-injected Logits Contrasting and Noise-injected Data, respectively.

| Methods | WebQA | | |
|---|--------------|--------------|--------------|
| | Single. | Multi. | Overall |
| RagLLaVA ($\eta = 0.5$) | 60.86 | 76.83 | 67.95 |
| w/o Reranker | 58.67 | 75.66 | 66.22 |
| w/o ND | 61.67 | 75.19 | 67.68 |
| w/o NLC | 60.08 | 76.24 | 67.26 |
| w/o ND & NLC | 60.68 | 74.92 | 67.01 |
| w/ Blended Reranker | 58.15 | 74.97 | 65.63 |

Results of Retrieval-augmented Generation Table 3 displays the results of multimodal question answering on two benchmark datasets requiring image retrieval. After applying our proposed pipeline, all configurations across the two experimental settings demonstrate excellent performance

of retrieval-augmented generation, approaching or even surpassing the performance of *Oracle*. When the natural threshold is activated, there is a significant increase in the accuracy of recalling the correct images (as shown in Table 2), leading to substantial improvements in all metrics across both datasets. This effect is even more pronounced when the adaptive threshold is activated. Moreover, this improvement is more evident in the single-image scenario. This is because we fixed the number of images recalled each time, and setting the threshold allows us to filter out erroneously recalled images, resulting in a consistent performance enhancement.

5.2 ABLATION STUDIES

To validate the efficacy of each component in our proposed method, we conduct a set of ablation experiments on WebQA, and the results are reported in Table 4.

Effect of Reranking For “*w/o Reranker*”, we directly retrieve Top-2 images with CLIP in the inference stage. For “*w/ Blended Reranker*”, we utilize the blended reranker for both reranking and generation, which is trained with noise-injected data and vanilla MLE loss. The use of the reranker in RagLLaVA shows an improvement in all metrics (*Single.*, *Multi.* and *Overall*) compared to “*w/o Reranker*”. The performance with the blended reranker is relatively poor, which is because training the blended reranker requires precise adjustments to the composition of the training datasets to achieve better results. In our case, we directly mix the ranking and QA datasets due to a lack of sufficient datasets, which leads to suboptimal performance.

Effect of Noise-injected Data For “*w/o ND*”, we replace the noise-injected dataset with the vanilla dataset. Ablating *ND* results in a performance decrease in *Multi.* and *Overall*, while the performance in *Single.* improves. Though introducing noise helps the model learn to distinguish between the candidate images more effectively in multi-image inference, additional candidates act as a form of fixed noise in single-image inference.

Effect of Noise-injected Logits Contrasting Since *NLC* enhances the model’s robustness at the token level, ablating it leads to a decrease in all metrics on WebQA. This decline is more pronounced when both *NLC* and *ND* are ablated, especially in multi-image inference scenarios. Therefore, our proposed training method, which injects noise at the data and token levels, demonstrates excellent performance.

5.3 RERANKING PERFORMANCE ANALYSIS

Effect of Captions To further verify the effectiveness of our proposed knowledge-enhanced ranking, we conduct experiments on test sets of WebQA ranking and QA datasets. In WebQA QA task, we retrieve top-20 candidate images using CLIP and rerank them into top-2 with our instruction-tuned reranker models. As shown in Table 5, the vanilla LLaVA-v1.5-13B performs poorly on both tasks. The models trained on the ranking task outperform the baseline, particularly the one trained on caption-aware task, which even surpasses CLIP-ViT-L/14-336px on *Recall@4* with its *Recall@2*. This demonstrates the superiority of our simple yet effective instruction templates in inducing the ranking ability of MLLMs.

Table 5: Reranking performance of different models on WebQA.

| Methods | WebQA Ranking | WebQA QA |
|----------------------------|---------------|------------------|
| | Acc | Recall@2 |
| LLaVA-v1.5-13B | 67.74 | 45.02 |
| <i>w/ Caption-agnostic</i> | 89.62 | 54.45 |
| <i>w/ Caption-aware</i> | 93.99 | 79.74 |
| CLIP-ViT-L/14-336px | - | 71.96 (Recall@4) |

6 CONCLUSION

In this paper, we present a robust framework for enhancing Multimodal Large Language Models (MLLMs) through knowledge-enhanced reranking and noise-injected training to tackle the multi-granularity noisy correspondence (MNC) problem in multimodal retrieval-augmented generation.

Our comprehensive approach addresses both coarse-grained and fine-grained noise, significantly improving retrieval accuracy and generation robustness. The results from our extensive experiments on the WebQA and MultimodalQA datasets demonstrate the superiority of our proposed method, especially in scenarios requiring fine-grained visual understanding and robust generation. By instruction-tuning MLLMs for reranking and injecting visual noise during training, we enhance the model’s capability to handle real-world noisy data and improve its overall performance in multimodal tasks.

REFERENCES

- Josh Achiam, Steven Adler, Sandhini Agarwal, Lama Ahmad, Ilge Akkaya, Florencia Leoni Aleman, Diogo Almeida, Janko Altenschmidt, Sam Altman, Shyamal Anadkat, et al. Gpt-4 technical report. *arXiv preprint arXiv:2303.08774*, 2023.
- Armen Aghajanyan, Bernie Huang, Candace Ross, Vladimir Karpukhin, Hu Xu, Naman Goyal, Dmytro Okhonko, Mandar Joshi, Gargi Ghosh, Mike Lewis, et al. Cm3: A causal masked multimodal model of the internet. *arXiv preprint arXiv:2201.07520*, 2022.
- Akari Asai, Zexuan Zhong, Danqi Chen, Pang Wei Koh, Luke Zettlemoyer, Hannaneh Hajishirzi, and Wen-tau Yih. Reliable, adaptable, and attributable language models with retrieval. *arXiv preprint arXiv:2403.03187*, 2024.
- Sebastian Borgeaud, Arthur Mensch, Jordan Hoffmann, Trevor Cai, Eliza Rutherford, Katie Millican, George Bm Van Den Driessche, Jean-Baptiste Lespiau, Bogdan Damoc, Aidan Clark, et al. Improving language models by retrieving from trillions of tokens. In *International conference on machine learning*, pp. 2206–2240. PMLR, 2022.
- Tom Brown, Benjamin Mann, Nick Ryder, Melanie Subbiah, Jared D Kaplan, Prafulla Dhariwal, Arvind Neelakantan, Pranav Shyam, Girish Sastry, Amanda Askell, et al. Language models are few-shot learners. *Advances in neural information processing systems*, 33:1877–1901, 2020.
- Yingshan Chang, Mridu Narang, Hisami Suzuki, Guihong Cao, Jianfeng Gao, and Yonatan Bisk. Webqa: Multihop and multimodal qa. In *Proceedings of the IEEE/CVF conference on computer vision and pattern recognition*, pp. 16495–16504, 2022.
- Wenhu Chen, Hexiang Hu, Xi Chen, Pat Verga, and William W Cohen. Murag: Multimodal retrieval-augmented generator for open question answering over images and text. *arXiv preprint arXiv:2210.02928*, 2022.
- Alexey Dosovitskiy, Lucas Beyer, Alexander Kolesnikov, Dirk Weissenborn, Xiaohua Zhai, Thomas Unterthiner, Mostafa Dehghani, Matthias Minderer, Georg Heigold, Sylvain Gelly, et al. An image is worth 16x16 words: Transformers for image recognition at scale. *arXiv preprint arXiv:2010.11929*, 2020.
- Matthijs Douze, Alexandr Guzhva, Chengqi Deng, Jeff Johnson, Gergely Szilvasy, Pierre-Emmanuel Mazaré, Maria Lomeli, Lucas Hosseini, and Hervé Jégou. The faiss library. 2024.
- Danny Driess, Fei Xia, Mehdi SM Sajjadi, Corey Lynch, Aakanksha Chowdhery, Brian Ichter, Ayzaan Wahid, Jonathan Tompson, Quan Vuong, Tianhe Yu, et al. Palm-e: An embodied multimodal language model. *arXiv preprint arXiv:2303.03378*, 2023.
- Yash Goyal, Tejas Khot, Douglas Summers-Stay, Dhruv Batra, and Devi Parikh. Making the v in vqa matter: Elevating the role of image understanding in visual question answering. In *Proceedings of the IEEE conference on computer vision and pattern recognition*, pp. 6904–6913, 2017.
- Ruiqi Guo, Philip Sun, Erik Lindgren, Quan Geng, David Simcha, Felix Chern, and Sanjiv Kumar. Accelerating large-scale inference with anisotropic vector quantization. In *International Conference on Machine Learning*, pp. 3887–3896. PMLR, 2020.
- Kelvin Guu, Kenton Lee, Zora Tung, Panupong Pasupat, and Mingwei Chang. Retrieval augmented language model pre-training. In *International conference on machine learning*, pp. 3929–3938. PMLR, 2020.

- Jonathan Ho, Ajay Jain, and Pieter Abbeel. Denoising diffusion probabilistic models. *Advances in neural information processing systems*, 33:6840–6851, 2020.
- Edward J Hu, Yelong Shen, Phillip Wallis, Zeyuan Allen-Zhu, Yuanzhi Li, Shean Wang, Lu Wang, and Weizhu Chen. Lora: Low-rank adaptation of large language models. *arXiv preprint arXiv:2106.09685*, 2021.
- Shaohan Huang, Li Dong, Wenhui Wang, Yaru Hao, Saksham Singhal, Shuming Ma, Tengchao Lv, Lei Cui, Owais Khan Mohammed, Barun Patra, et al. Language is not all you need: Aligning perception with language models. *Advances in Neural Information Processing Systems*, 36, 2024.
- Zhenyu Huang, Guocheng Niu, Xiao Liu, Wenbiao Ding, Xinyan Xiao, Hua Wu, and Xi Peng. Learning with noisy correspondence for cross-modal matching. *Advances in Neural Information Processing Systems*, 34:29406–29419, 2021.
- Drew A Hudson and Christopher D Manning. Gqa: A new dataset for real-world visual reasoning and compositional question answering. In *Proceedings of the IEEE/CVF conference on computer vision and pattern recognition*, pp. 6700–6709, 2019.
- Gautier Izacard and Edouard Grave. Leveraging passage retrieval with generative models for open domain question answering. *arXiv preprint arXiv:2007.01282*, 2020.
- Vladimir Karpukhin, Barlas Oğuz, Sewon Min, Patrick Lewis, Ledell Wu, Sergey Edunov, Danqi Chen, and Wen-tau Yih. Dense passage retrieval for open-domain question answering. *arXiv preprint arXiv:2004.04906*, 2020.
- Sicong Leng, Hang Zhang, Guanzheng Chen, Xin Li, Shijian Lu, Chunyan Miao, and Lidong Bing. Mitigating object hallucinations in large vision-language models through visual contrastive decoding. In *Proceedings of the IEEE/CVF Conference on Computer Vision and Pattern Recognition*, pp. 13872–13882, 2024.
- Patrick Lewis, Ethan Perez, Aleksandra Piktus, Fabio Petroni, Vladimir Karpukhin, Naman Goyal, Heinrich Küttler, Mike Lewis, Wen-tau Yih, Tim Rocktäschel, et al. Retrieval-augmented generation for knowledge-intensive nlp tasks. *Advances in Neural Information Processing Systems*, 33: 9459–9474, 2020.
- Junnan Li, Dongxu Li, Silvio Savarese, and Steven Hoi. Blip-2: Bootstrapping language-image pre-training with frozen image encoders and large language models. In *International conference on machine learning*, pp. 19730–19742. PMLR, 2023.
- Xi Victoria Lin, Xilun Chen, Mingda Chen, Weijia Shi, Maria Lomeli, Rich James, Pedro Rodriguez, Jacob Kahn, Gergely Szilvasy, Mike Lewis, et al. Ra-dit: Retrieval-augmented dual instruction tuning. *arXiv preprint arXiv:2310.01352*, 2023.
- Haotian Liu, Chunyuan Li, Yuheng Li, and Yong Jae Lee. Improved baselines with visual instruction tuning. In *Proceedings of the IEEE/CVF Conference on Computer Vision and Pattern Recognition*, pp. 26296–26306, 2024a.
- Haotian Liu, Chunyuan Li, Qingyang Wu, and Yong Jae Lee. Visual instruction tuning. *Advances in neural information processing systems*, 36, 2024b.
- Pan Lu, Liang Qiu, Kai-Wei Chang, Ying Nian Wu, Song-Chun Zhu, Tanmay Rajpurohit, Peter Clark, and Ashwin Kalyan. Dynamic prompt learning via policy gradient for semi-structured mathematical reasoning. *arXiv preprint arXiv:2209.14610*, 2022.
- Kenneth Marino, Mohammad Rastegari, Ali Farhadi, and Roozbeh Mottaghi. Ok-vqa: A visual question answering benchmark requiring external knowledge. In *Proceedings of the IEEE/cvf conference on computer vision and pattern recognition*, pp. 3195–3204, 2019.
- Brandon McKinzie, Zhe Gan, Jean-Philippe Fauconnier, Sam Dodge, Bowen Zhang, Philipp Dufter, Dhruvi Shah, Xianzhi Du, Futang Peng, Floris Weers, et al. Mm1: Methods, analysis & insights from multimodal llm pre-training. *arXiv preprint arXiv:2403.09611*, 2024.

- Anand Mishra, Shashank Shekhar, Ajeet Kumar Singh, and Anirban Chakraborty. Ocr-vqa: Visual question answering by reading text in images. In *2019 international conference on document analysis and recognition (ICDAR)*, pp. 947–952. IEEE, 2019.
- Alec Radford, Jong Wook Kim, Chris Hallacy, Aditya Ramesh, Gabriel Goh, Sandhini Agarwal, Girish Sastry, Amanda Askell, Pamela Mishkin, Jack Clark, et al. Learning transferable visual models from natural language supervision. In *International conference on machine learning*, pp. 8748–8763. PMLR, 2021.
- Colin Raffel, Noam Shazeer, Adam Roberts, Katherine Lee, Sharan Narang, Michael Matena, Yanqi Zhou, Wei Li, and Peter J Liu. Exploring the limits of transfer learning with a unified text-to-text transformer. *Journal of machine learning research*, 21(140):1–67, 2020.
- Aditya Ramesh, Mikhail Pavlov, Gabriel Goh, Scott Gray, Chelsea Voss, Alec Radford, Mark Chen, and Ilya Sutskever. Zero-shot text-to-image generation. In *International conference on machine learning*, pp. 8821–8831. Pmlr, 2021.
- Ramprasaath R Selvaraju, Michael Cogswell, Abhishek Das, Ramakrishna Vedantam, Devi Parikh, and Dhruv Batra. Grad-cam: Visual explanations from deep networks via gradient-based localization. In *Proceedings of the IEEE international conference on computer vision*, pp. 618–626, 2017.
- Alon Talmor, Ori Yoran, Amnon Catav, Dan Lahav, Yizhong Wang, Akari Asai, Gabriel Ilharco, Hannaneh Hajishirzi, and Jonathan Berant. Multimodalqa: Complex question answering over text, tables and images. *arXiv preprint arXiv:2104.06039*, 2021.
- Anthony Meng Huat Tiong, Junnan Li, Boyang Li, Silvio Savarese, and Steven CH Hoi. Plug-and-play vqa: Zero-shot vqa by conjoining large pretrained models with zero training. *arXiv preprint arXiv:2210.08773*, 2022.
- Hugo Touvron, Thibaut Lavril, Gautier Izacard, Xavier Martinet, Marie-Anne Lachaux, Timothée Lacroix, Baptiste Rozière, Naman Goyal, Eric Hambro, Faisal Azhar, et al. Llama: Open and efficient foundation language models. *arXiv preprint arXiv:2302.13971*, 2023.
- Xin Xiao, Bohong Wu, Jiacong Wang, Chunyuan Li, Xun Zhou, and Haoyuan Guo. Seeing the image: Prioritizing visual correlation by contrastive alignment. *arXiv preprint arXiv:2405.17871*, 2024.
- Qian Yang, Qian Chen, Wen Wang, Baotian Hu, and Min Zhang. Enhancing multi-modal multi-hop question answering via structured knowledge and unified retrieval-generation. In *Proceedings of the 31st ACM International Conference on Multimedia*, pp. 5223–5234, 2023.
- Xi Ye and Greg Durrett. The unreliability of explanations in few-shot prompting for textual reasoning. *Advances in neural information processing systems*, 35:30378–30392, 2022.
- Jiahui Yu, Yuanzhong Xu, Jing Yu Koh, Thang Luong, Gunjan Baid, Zirui Wang, Vijay Vasudevan, Alexander Ku, Yinfei Yang, Burcu Karagol Ayan, et al. Scaling autoregressive models for content-rich text-to-image generation. *arXiv preprint arXiv:2206.10789*, 2(3):5, 2022.